

Casopitant: in-vitro data and SimCyp™ simulation to predict in-vivo metabolic interactions involving Cytochrome P450 3A4

Authors:

Paola Motta, Nicoletta Pons, Sabrina Pagliarusco, Mario Pellegatti and

Fiorenza Bonomo

Department of Drug Metabolism and Pharmacokinetics, Medicine Research

Center, GlaxoSmithKline, Verona, Italy

RUNNING TITLE

a) IVIVE of Casopitant for DDIs involving CYP3A4.

b) Paola Motta, DMPK Aptuit Verona S.r.l., Via Fleming 4 37135 Verona,
tel +39 0458219602, fax +39 0458218055, e-mail paolamottait@yahoo.it or
paola.motta@aptuit.com

c) Number of Text pages: 40

Number of Tables: 8

Number of Figures: 4

Number of References: 28

Number of words in Abstract: 246 words

Number of words in Introduction: 511 words

Number of words in Discussion: 1408 words

d) Abbreviations used are:

$6\beta T$ = 6β -hydroxy testosterone

AUC = Area under the plasma concentration-time curve

C_{max} = Maximal plasma concentration

Cl_{int} = Intrinsic clearance

CYP = Cytochrome P450

DDI = Drug-drug interaction

DMPK = Drug metabolism and pharmacokinetics

DMSO = Dimethyl sulfoxide

f_m = fraction substrate eliminated by a single (CYP) pathway

GW679769 = 1-piperidinecarboxamide,4-(4-acetyl-1-piperazinyl)-N-

((1R)-1-(3,5-bis(trifluoromethyl)phenyl)-ethyl)-2-(4-fluoro-2-methylphenyl)-N-methyl-
(2R,4S)

HLM = Human liver microsomes

HPLC-MS/MS = High performance liquid chromatography with tandem mass
spectroscopy

IC₅₀ = Concentration that would cause a 50% decrease in CYP activity

IVIV = In Vitro - In Vivo

KET = Ketoconazole

k_{inact} = The maximum rate of inactivation at saturation

K_I = Concentration required for half-maximal inactivation

MID = Midazolam

MRM = Multiple reaction monitoring

NADPH = Nicotinamide adenine dinucleotide phosphate-reduced form

NIF = Nifedipine

OME = Omeprazole

PB = Phenobarbital

RIF = Rifampin

t_{max} = Time to reach C_{max}

TAO = Troleandomycin

V_{ss} = Steady-state volume of distribution

ABSTRACT

Casopitant has previously been shown to be a potent and selective antagonist of the human neurokinin-1 receptor, the primary receptor of substance P, both in vitro and in vivo, with good brain penetration properties. Based on this mode of action it was evaluated for the prevention of chemotherapy-induced and post-operative nausea and vomiting, and for the chronic treatment of anxiety, depression, insomnia, and over-active bladder. Casopitant is shown to be a substrate, an inhibitor and an inducer of cytochrome P450 (CYP) 3A4 and, because of this complex behavior, it was difficult to identify the primary mechanism by which it may give rise to drug-drug interactions (DDIs) of clinical relevance. Moreover, the major circulating metabolite is itself an inhibitor of CYP3A4 in vitro. Based on the different clinical indications and the various potential co-medications of casopitant, a relevant part of the clinical development plan was focused on the assessment of the importance of clinical DDIs. The present study provides an overview of the DDI potential profile of casopitant, based on in vitro data and clinical evidences of its interaction with CYP3A4 probe substrates midazolam (MID) and nifedipine (NIF), the strong inhibitor ketoconazole (KET) and the inducer rifampin (RIF). Overall, the clinical data confirm the ability of casopitant to interact with CYP3A4 substrates, inhibitors or inducers. The in vitro data are enough accurate and robust to build a reliable SimCypTM population-based model, so as to estimate the potential DDI of casopitant and to minimize the clinical studies recommended.

INTRODUCTION

DDIs have become an important issue in health care. It is now acknowledged that many of the major pharmacokinetic DDIs can be attributed to modulations of the drug-metabolizing enzymes, particularly CYP enzymes, which are present in the liver and extra-hepatic tissues (Bibi, 2008). CYP3A4 is the most abundantly expressed CYP enzyme in the liver and gut, and it is involved in the clearance of more than half of the drugs used clinically (Wienkers and Heath, 2005). A number of important drugs have been identified as substrates, inducers, and/or inhibitors of CYP3A4 and the assessment of the potential for CYP3A4 mediated DDIs is an important part of the clinical development program for any new chemical entity (Hewitt, 2007).

Casopitant (Figure 1), also known as GW679769 [1-piperidinecarboxamide,4-(4-acetyl-1-piperazinyl)-N-((1R)-1-(3,5-bis(trifluoromethyl)phenyl)-ethyl)-2-(4-fluoro-2-methylphenyl)-N-methyl-(2R,4S)], is a piperidine derivative with potent and selective antagonistic properties towards the human neurokinin-1 receptor and good brain penetration properties (Minthorn, 2008). It has been evaluated in humans for chemotherapy-induced nausea and vomiting (Herrstedt, 2009), post-operative nausea and vomiting, anxiety, depression, insomnia, and over-active bladder. Based on in vivo clinical data, casopitant is extensively metabolized and its metabolism in human appears to be mediated mainly by CYP3A4 (Pellegatti, 2009; Johnson, 2010). GSK525060 (Figure 1), the major circulating metabolite in man, is present at concentrations comparable to those of the parent drug, both after single (Pellegatti, 2009) and repeated (Zamuner, 2010) oral administration of casopitant.

Given the different therapeutic indications of this drug, many of which may require various co-medications, an assessment of the potential DDI profile for casopitant was important to determine whether it could be safely added to an ongoing therapy and at what dose. In order to assess potential for DDIs, knowledge of clearance mechanisms, enzyme responsible for major metabolic pathways, and modulating capabilities of enzyme activities was essential. Consequently, several in vitro studies were performed in order to evaluate the potential of casopitant or GSK525060 as perpetrator and as victim of metabolic interactions involving CYP3A4 and to guide the clinical DDI strategy. This study describes the in vitro data obtained and used to build reliable SimCyp™ model to estimate the potential DDI of casopitant. These simulations were then compared to clinical DDI results already available for casopitant when co-administered with the CYP3A4 probes MID or NIF, and with KET or RIF. This retrospective analysis was essential to properly evaluate the reliability of the SimCyp™ predictions and their potential future use in drug development to minimize the clinical DDI studies recommended based on in vitro data.

The importance of prediction and evaluation of DDIs has been reinforced by some guidelines currently under revision by regulatory authorities (FDA, <http://www.fda.gov/downloads/Drugs/GuidanceComplianceRegulatoryInformation/Guidances/ucm072101.pdf>); and EMA, http://www.ema.europa.eu/docs/en_GB/document_library/Scientific_guideline/2010/05/WC500090112.pdf). The development and refinement of computer-based simulation models represent, thus, a powerful tool to predict quantitatively and accurately clinically important DDIs and to improve decision making in drug development and discovery. In

particular, with the SimCypTM approach, the combined knowledge of in vitro DDI data and clinical pharmacokinetics of the drug can be used to simulate various clinical drug interaction scenarios and to identify an efficient and effective clinical plan strategy (Fahmi, 2009).

MATERIALS AND METHODS

Chemicals and reference compounds

The test (articles) compounds were obtained from the following sources: casopitant (GW679769), GSK525060 (Figure 1), and all the bioanalytical internal standards from GlaxoSmithKline; MID, NIF, KET, troleandomycin (TAO), hydroxytriazolam, glucose-6-phosphate, and glucose-6-phosphate dehydrogenase from Sigma-Aldrich (Milan, Italy); 1'-hydroxy midazolam and oxidized nifedipine from BD Biosciences (Bedford, MA, USA). Human liver microsomes (HLM) pooled from 15 donors were prepared and characterized at XenoTech LLC (Lenexa, KS, USA). BactosomesTM containing individual overexpressed human CYP3A4 (derived from baculovirus infected cells) were obtained from Cypex Ltd. (Dundee, UK). RIF, phenobarbital (PB), omeprazole (OME), testosterone, 6 β -hydroxytestosterone (6 β T), as well as freshly isolated human hepatocytes were provided by CellsDirect.

All other reagents and solvents were of the highest purity available and were obtained from commercial sources.

In vitro studies

Preparations

1. In vitro Cytochrome P450 induction

The human hepatocyte model was used as experimental system for the evaluation of P450 induction potential to predict clinical DDIs as reported by Fahmi, 2008. Fresh human hepatocytes from three separate donors were isolated and cultured essentially as described by Maurel, 1996 and LeCluyse, 2001. After a 24-48 hours adaptation period, cultures of hepatocytes with a Matrigel[®] overlay were treated for 3 consecutive days with casopitant (1, 5, or 20 μ M) once daily; or, alternatively, with one of three prototypical P450 inducers, OME (25 μ M), PB (500 μ M), and RIF (10 μ M) again given once a day for 3 consecutive days. Casopitant and inducers (positive controls) were dissolved in Dimethyl Sulfoxide (DMSO), and hepatocytes treated with DMSO (final concentration 0.1%, v/v) served as negative controls. Human hepatocytes were harvested after the final treatment to prepare microsomes, which were tested in duplicates for CYP3A4 activity (testosterone 6 β -hydroxylation) by High Performance Liquid Chromatography with tandem Mass Spectroscopy (HPLC-MS/MS), according to the procedure reported by Madan, 2003.

Data analysis: Rates of production of 6 β T were calculated at each concentration of casopitant or prototypical inducer and expressed as nmol/min/mg. Each hepatocytes donor preparation was deemed acceptable when the RIF positive control elicited a greater than 2-fold increase in the CYP enzyme activity (Sinz, 2008). The inductive response of casopitant on CYP3A4 activity was expressed as mean ratio of treated over vehicle control (fold change) or compared with the appropriate prototypical inducer as percent of positive control (RIF), according to the following equations:

$$\text{Fold change} = \left(\frac{\text{mean CYP3A4 activity in treated cells}}{\text{mean CYP3A4 activity in solvent control}} \right)$$

$$\% \text{Max} = \left(\frac{(\text{Casopitant mean CYP3A4 activity} - \text{solvent control mean CYP3A4 activity})}{(\text{prototypical inducer mean CYP3A4 activity} - \text{solvent control mean CYP3A4 activity})} \right) * 100$$

2. *In vitro* Cytochrome P450 inhibition

IC₅₀ determination: Unless indicated otherwise, CYP3A4 activity in HLM was determined according to previously published procedures (Madan, 2002) and the concentration that would cause a 50% decrease in CYP activity (IC₅₀) determined. Incubations were conducted in 250 μL incubation mixture (pH 7.4) containing 50 mM potassium phosphate buffer, pooled HLM (0.1 mg/ml), probe substrates (2.5 μM MID or 10 μM NIF) and casopitant or GSK525060 (concentration range 0.1-100 μM). All incubations were pre-warmed at 37°C for 5 minutes before the addition of pre-warmed NADPH-generating system so as to obtain the following final concentrations: NADP 5.5 mM; glucose-6-phosphate 0.4 mM and 1.2 units of glucose-6-phosphate dehydrogenase per ml. Reactions were terminated after 5 minutes for MID or 10 minutes for NIF by the addition of acetonitrile and the production of metabolite in each incubation was quantified by HPLC-MS/MS.

To evaluate the potential for metabolism-dependent inhibition, casopitant or GSK525060 (at the same concentrations used to evaluate direct inhibition), were pre-incubated at 37°C with HLM and a NADPH-generating system (see above) or probe substrates (2.5 μM MID or 10 μM NIF) for 20 minutes. Reactions were then initiated by the addition of marker substrates or NADPH-generating system, respectively, and the incubations were

continued for 5 or 10 minutes to measure the residual CYP3A4 activity. Reactions were terminated by the addition of acetonitrile and the production of metabolite in each incubation was quantified by HPLC-MS/MS.

Positive control incubations for both direct (KET) and metabolism-dependent inhibition (TAO) and control incubations without inhibitor (containing methanol only) were also performed. All incubations were performed in duplicates and prepared such that the final concentration of methanol was constant at 2% (v/v).

K_I and k_{inact} determination: The recommended two-step incubation method was employed to determine the kinetics of CYP3A4 inactivation by casopitant (Polasek and Miners, 2007; Yang, 2005), the concentration required for half-maximal inactivation (K_I) and the maximum rate of inactivation at saturation (k_{inact}).

Various concentrations of casopitant (0.9-90 μ M) were pre-warmed at 37°C in 0.1 M Tris buffer pH 7.4 with 0.5 mM EDTA and pooled HLM (0.5 mg/ml). Following 5 minutes pre-warming, the NADPH generating system was added and the mixture incubated for 0 to 20 minutes. After pre-incubation, aliquots (25 μ l) were transferred to dilution mix wells (225 μ l) containing 0.1 M Tris buffer pH 7.4 with 0.5 mM EDTA, 28 μ M MID and NADPH-generating system. Reactions were terminated after 4 minutes incubation with 250 μ l acetonitrile and the production of metabolite in each incubation quantified by HPLC-MS/MS. With the transfer into the dilution mix step, microsomes were diluted 1:10 to a 0.05 mg/ml final concentration of protein and casopitant underwent a similar dilution. Positive control incubations (TAO) and control incubations without inhibitor (containing methanol only) were also performed. All incubations were performed in

duplicates and prepared such that the final concentration of methanol was constant at 2% (v/v).

Data analysis: Rates of metabolite production at each concentration of casopitant, GSK525060 or positive control were expressed as a percentage of the mean uninhibited control rate for each incubation. Data were processed to determine IC₅₀ values by non-linear regression with GraFit (version 5.0, Erithacus Software, Horley, Surrey, UK) according to the following equation:

$$v = \frac{V_0}{1 + \left(\frac{[I]}{IC_{50}} \right)^s}$$

where V₀ = uninhibited control rate of metabolite production, v = observed rate of metabolite production, [I] = inhibitor concentration, s = slope factor. Metabolism-dependent inhibition of enzyme activity was inferred from a decrease (> 2-fold) in IC₅₀ value obtained following the 20 minute NADPH pre-incubation relative to that obtained with the probe substrate pre-incubation.

Data for the K_I and k_{inact} investigation were analyzed to determine the rate of enzyme inactivation at each casopitant concentration tested (Polasek and Miners, 2007), assuming the loss of enzyme activity due to inactivation by a first-order process. For each NADPH pre-incubation period, rates of 1'-hydroxymidazolam production at each concentration of casopitant, or of the positive control TAO, were expressed as a percentage of the mean uninhibited control rate. Rate constants for loss of CYP3A4 activity, at each inhibitor concentration, were calculated according to a single exponential decay equation using GraFit:

$$v = V_0 e^{-k_{obs}t}$$

where v = observed rate of metabolite production, V_0 = initial rate of metabolite production, k_{obs} = observed rate constant and t = NADPH pre-incubation period. Data were then processed to determine the kinetic constants, k_{inact} and K_I , by non-linear regression with GraFit according to the following equation..

$$k_{obs} = \frac{k_{inact}[I]}{K_I + [I]}$$

3. Metabolism of casopitant by human liver microsomes and recombinant human CYP3A4

Microsomal incubations (HLM or recombinant CYP3A4) were performed under the conditions described in Madan, 2002 (in an incubation mixture containing 50 mM phosphate buffer, pH 7.4. and a NADPH-generating system), and the rate of formation of GSK525060 was determined under conditions where the reaction was linear with time and protein concentration. Initial studies were conducted in HLM with two concentrations of casopitant (5 μ M and 20 μ M) to optimize the incubation time (over the range 0-90 minutes at 1 mg/ml protein concentration) and protein concentration (over the concentration range 0.05-5 mg/ml at 30 minutes); with recombinant CYP3A4 and casopitant 10 μ M, to determine reaction linearity with respect to CYP content (over the concentration range 10-250 pmol/ml). Experiments to determine enzyme kinetics were performed over 30 minute incubation time at a microsomal protein concentration of 1 mg/ml or at 100 pmol CYP/ml with casopitant final concentration ranging from 0.1 to

50 μ M. All kinetics incubations were performed in triplicates and rates of GSK525060 formation were quantified by HPLC-MS/MS.

Data analysis: GSK525060 formation was calculated as picomoles of metabolite produced per picomoles CYP/hour. Linear and non-linear regression analysis of data was performed using Grafit. Kinetic parameters (K_m and V_{max}) for casopitant metabolism were calculated according to the Michaelis-Menten equation.

$$V = \frac{V_{max} [S]}{K_m + [S]}$$

where: v = observed rate of metabolite production; V_{max} = maximal rate of metabolite production; $[S]$ = casopitant concentration; K_m = concentration of casopitant required to achieve half-maximal rate.

Linearization plots were calculated by using Lineweaver-Burk linearization equation:

$$1/v = K_m/V_{max} [S] + 1/V_{max}$$

Bioanalytical methods: Measurements of casopitant metabolite, GSK525060, 6 β T, 1'-hydroxy midazolam and oxidized nifedipine from in vitro incubations were performed with validated and specific HPLC-MS/MS assay by or on behalf of Drug metabolism and pharmacokinetics (DMPK) Department, GlaxoSmithKline. The bioanalytical methods are based upon internal standard addition after protein precipitation with acetonitrile, centrifugation and subsequent injection onto a HPLC-MS/MS system for analysis employing a positive-ionization mode. TurboIonSpray ionization and multiple reactions monitoring (MRM) was conducted on an Applied Biosystem API-4000 mass spectrometer (Applied Biosystem/MDS-Sciex, Concord, Ontario, Canada) to ensure high selectivity. The characteristic precursor $[MH]^+$ to product ions transitions monitored in

MRM are consistent with the structures of GSK525060, 6 β T, 1'-hydroxy midazolam, oxidized nifedipine and their internal standards.

The selectivity of the methods was confirmed by the inclusion of blank and double blank samples prepared from pooled HLM in validation assays. The precision (relative standard deviation) and accuracy (relative error) in pooled HLM, was derived from the analysis of replicates validation samples (n=6) at 5 concentrations for each analyte. At all concentrations examined of these validation sample, the intra-day precision value for casopitant metabolite GSK525060, and for 6 β T, or the inter-day precision value for 1'-hydroxy midazolam and oxidized nifedipine were both less than or equal to 15%, and so was the accuracy of assay of the casopitant metabolite, GSK525060, 6 β T, 1'-hydroxy midazolam and oxidized nifedipine. Both precision and accuracy were therefore considered acceptable (FDA, <http://www.fda.gov/downloads/Drugs/GuidanceComplianceRegulatoryInformation/Guidances/UCM070107.pdf>).

For GSK525060 determination in microsomal homogenate, the method was validated over the concentration range 6 to 6000 ng/ml using HPLC-MS/MS. Samples were chromatographed on a Hypersil Gold column (50x3 mm, 5 μ m, Thermo Scientific) with a mobile phase 5 mM ammonium acetate/acetonitrile 35:65 (v/v), at a flow rate of 0.7 ml/min.

The method of 6 β T determination in microsomal homogenate was validated over the concentration range 5.00 to 5000 ng/ml using HPLC-MS/MS. Samples were chromatographed on a Hypersil ODS (150x4.6mm, 5 μ m, Thermo Scientific), with a mobile phase A (methanol/acetonitrile, 98:2 v/v) and B (water/acetonitrile, 98:2 v/v), at a

flow rate of 1 ml/min, using a stepped elution (0-10 min 43% A/57% B, 10-20 min 43 % A/57% B to 73% A/27% B, 20-30 min 73% A/27% B, 30-36 min 73% A/27% B to 43% A/57% B, 36-41 min 43% A/57% B).

The methods of analyte determination in microsomal homogenate were validated over the concentration range 1 to 1000 nM for 1'-hydroxy midazolam, and 5 to 5000 nM for oxidized nifedipine. Samples were chromatographed on a MetaChem Inertsil ODS-3, (33x3 mm, 3 μ m GL Science Inc.), with mobile phase A (0.1% formic acid, aqueous) and B (acetonitrile), at a flow rate of 0.6 ml/min, using a stepped elution for 1'-hydroxy midazolam (0-0.5.0 min 95% A/5% B to 50% A/50% B, 0.50-0.52 min 50% A/50% B, 0.52-1.10 50% A/50% B to 10% A/90% B, 1.10-1.20 min 10% A/90% B, 1.20-1.21 min 10% A/90% B to 95% A/5% B, 1.21-2.10 95% A/5% B) and an isocratic gradient for oxidized nifedipine (0-2.8 min 55% A/45% B).

Calibration plots of analyte/internal standard peak area ratio versus marker metabolite concentration were constructed and a weighted $1/x^2$ linear regression applied to the data. Quality Control samples (QC), prepared at 3 different analyte concentrations and stored alongside the samples under study, were analyzed with each batch of samples against separately prepared calibration standards. For the analysis to be acceptable, no more than one-third of the total QC results and no more than one-half of the results from each concentration level were to deviate from the nominal concentration by more than 15%.

SimCypTM Simulations: The physicochemical and pharmacokinetic characteristics for casopitant, together with the kinetic parameters generated in vitro, were entered into SimCypTM (version 9.03) to create a new “inhibitor” profile. Input parameters for casopitant, shown in the Table 1, were calculated in-house from in vitro and in vivo

experimental data, while the CYP3A4 inhibitor (KET), CYP3A4 inducer (RIF) or CYP3A4 substrates (MID and NIF) input data were supplied by the program.

Before starting the DDI predictions of casopitant as the victim or perpetrator, the plasma concentration time profile and pharmacokinetics parameters for a single oral dose of casopitant at 100 mg was simulated using a one compartment distribution model and intrinsic clearance value (Cl_{int}) (Enzyme kinetics options), calculated in-house from the K_m and V_{max} values of GSK525060 production, as measured in HLM incubations. The assumptions were made that all casopitant metabolism was due to CYP3A4 and that GSK525060 was the only or the major metabolite of casopitant (Pellegatti, 2009), but no parameters for GSK525060 were included in the SimCyp™ for the simulation.

For MID and NIF the model options applied were the oral route, the first order absorption model, one compartment model for distribution and enzyme kinetic option for elimination.

The impact of casopitant on the DDI was evaluated as perpetrator and victim. As perpetrator, the simulations were performed with two CYP3A4 substrates, MID and NIF, applying the clinical trial design. Virtual trial were run for a single oral dose of 5.0 mg MID (taken at 10:00, fasted) or 10 mg NIF (taken at 9:00, fasted) with or without casopitant (given at 9:00, fasted) at repeated dose of 30, or 120 mg/day. The drug co-administration occurred after 3 or 14 days of casopitant treatment. The magnitude of the interaction was expressed as the increase in exposure of MID or NIF, as mean area under the plasma-concentration-time curve (AUC). To assess the impact of trial design and inter individual variability on the interaction, the simulations were performed using this set of inactivation data: 10 trials of healthy volunteers comprising 10 subjects (20-50 years, 1:1

male/female ratio). The degree of inter-individual variability in simulations was investigated using frequency histograms of AUC ratio.

As victim, the simulations were performed with KET, a CYP3A4 inhibitor, and RIF, a CYP3A4 inducer, using the same virtual population and trial design described above and both time-dependent and steady state conditions. The time-dependent model accounts for time- and concentration- dependent enzyme inhibition applying the actual study design used in the clinical DDI studies. The steady-state simulation was run to evaluate the maximum potential for interaction where both victim and perpetrator were at steady-state concentrations. Virtual trials were run for repeat dose of KET at 400 mg for seven days and at the Day 4, when casopitant was dosed at 100 mg at the same time with KET administration. The simulations with RIF were performed dosing RIF at 600 mg for nine days and casopitant also given as a single dose of 150 mg on Day 8 at the same time of RIF administration.

In vivo studies

Designs and treatments

Interaction with Midazolam: GSK study NKF10011 was a single center, open-label study to evaluate the potential pharmacokinetic interaction in healthy subjects of repeated daily oral doses of 30 mg, or 120 mg casopitant and single doses of 5 mg oral MID. Oral casopitant was administered for 14 days (study Days 8 to 21) to two cohorts of 16 subjects each. Midazolam (HYPNOVEL, Roche; 1 ml of 5 mg/ml solution) was administered alone as single dose on Day 1; and 1 hour after casopitant on Days 10 and 21. The time of administration was chosen to match the maximal plasma concentrations

of the two drugs and, thus, maximize the potential pharmacokinetic interaction. This allowed a comparison of the pharmacokinetics of MID, when this drug was given on its own, or after 3 and 14 days of daily treatment with casopitant (Zamuner, 2010).

Interaction with Nifedipine: GSK study NKF10012 was a single center, open-label study to evaluate the potential interaction in healthy subjects between repeated daily oral doses of 30 mg, or 120 mg/day casopitant and a single dose of 10 mg oral NIF. Oral casopitant was administered for 14 days (study Days 8 to 21) to two cohorts, with 13 to 14 subjects each. Both cohorts received a single oral dose of 10 mg nifedipine (ADALAT, Bayer Healthcare AG, Germany) on Day 1. On Day 8 all subjects commenced a 14-days treatment with daily oral doses of casopitant. On Days 10 and 21, all subjects also received a single 10 mg oral dose of NIF. This allowed a comparison of the pharmacokinetics of NIF, when this drug was given on its own, or after 3 and 14 days of daily treatment with casopitant (Zamuner, 2010).

In both studies, blood samples for determination of plasma concentration of MID or NIF, casopitant and its metabolite GSK525060 were collected at selected days and time-points and analyzed by HPLC-MS/MS (Zamuner, 2010).

Interaction with Ketoconazole: GSK study NKV105093 was an open-label study to evaluate in healthy subjects the potential interaction of repeated daily oral doses of 400 mg ketoconazole (Nizoral, Janssen Pharmaceutica Inc.) with a single oral dose of 100 mg casopitant. Oral KET was administered for 7 days (study Days 9 to 15) to 12 subjects. Oral casopitant was administered alone as single dose of 100 mg on Day 1; and administered together with KET on Day 12 (Johnson, 2010).

Interaction with Rifampin: GSK study NKV105091 was an open-label study to evaluate in healthy subjects the potential interaction of repeated single daily doses of 600 mg oral rifampin (RIFADIN, rifampin capsules, USP) with oral casopitant given as a single dose of 150 mg. Oral RIF was administered for 7 days (study Days 9 to 17) to 12 subjects. Oral casopitant, as a single dose of 150 mg was administered alone on Day 1; and together with RIF on Day 16 (Johnson, 2010).

For both studies of interaction of casopitant with KET and RIF, blood samples for determination of plasma concentration of casopitant and its metabolite GSK525060 were collected at selected time-points and analyzed by HPLC-MS/MS (Johnson, 2010).

Bioanalytical methods

Measurements of casopitant, its metabolite GSK525060, MID, NIF, KET, and RIF in plasma were performed with validated and specific HPLC-MS/MS assay by or on behalf of DMPK, GlaxoSmithKline. All the details of the bioanalytical methods and their specific performances are reported in Zamuner, 2010; and Johnson, 2010.

Pharmacokinetic analysis

Pharmacokinetic analysis applied to the concentration-time profiles concerning casopitant, GSK525060, MID, and NIF, is reported in Zamuner, 2010; and Johnson, 2010.

RESULTS

In vitro data

Cytochrome P450 induction

The increased CYP3A4 activity (measured as testosterone 6 β -hydroxylation) observed in human hepatocytes after exposure to the inducers suggested that greater amounts of enzyme were present as result of the induction. In particular, the positive control RIF yielded a 2.1-fold, a 13-fold, and a 6.0-fold increase in activity, as compared to the vehicle control activities, in donors 1, 2 and 3, respectively (Table 2) which is consistent with literature data (Luo, 2002; Madan, 2003). Although the magnitude of CYP3A4 induction was quite variable among the three hepatocyte preparations, these data indicated clearly that the hepatocytes in culture were responding appropriately for at least two out of three donors.

A similar, but less potent, pattern of CYP3A4 enzyme induction was observed in hepatocyte cultures treated with casopitant, especially in cells from donors 2 and 3, the ones which had responded more markedly to RIF. The slight decrease in the CYP3A4 activity observed at 20 μ M compared to 5 μ M may be due to the fact that casopitant and its metabolite are also inhibitors/inactivators of CYP3A4. Cytotoxicity of casopitant at this concentration was not likely, as this decrease was not observed on the other CYPs activities tested on the same human hepatocyte preparations (data not shown).

Cytochrome P450 inhibition

The ability of casopitant and its metabolite GSK525060 to inhibit CYP3A4 metabolism of probe substrates (MID and NIF), in a direct and metabolism-dependent manner, was

investigated in pooled HLM and the results are summarized in Table 3. Both casopitant and GSK525060 were shown to inhibit CYP3A4 activity, as measured with both probe substrates, with an IC_{50} lower than 10 μ M. Moreover, pre-incubation of casopitant or its metabolite with HLM in the presence of NADPH did increase their inhibitory effects, suggesting that both drugs behaved also as metabolism-dependent inhibitors of CYP3A4. In particular, the decreases in IC_{50} for casopitant and GSK525060 in the metabolism of MID were characterized by IC_{50} shifts of approximately 4.3 and 3.0-fold, respectively. Metabolism-dependent inhibition of CYP3A4 by casopitant was further investigated, and the inactivation parameter k_{inact} and K_I determined using MID as probe substrate. The results and associated kinetic plots are shown in Figure 2. Casopitant showed a progressive increase in inhibitory potency with increasing NADPH pre-incubation time and concentration. This increase in potency was characteristic of a metabolism-dependent inhibitor which requires enzymatic activation and, therefore, the presence of NADPH. The kinetic constants for the inactivation of CYP3A4 were determined to be 0.0199 min^{-1} (k_{inact}) and 3.10 μ M (K_I) by casopitant, and 0.0468 min^{-1} (k_{inact}) and 0.35 μ M (K_I) by TAO. The relative inactivation efficiency on CYP3A4 activity of the test control TAO, presented by the ratio $k_{inact}/K_I=0.13$, is in agreement with the data reported by Xu, 2009 and confirms the validity of this assay.

Metabolism of casopitant by HLM and recombinant human CYP3A4

The formation of GSK525060 was found to be linear with time up to 30 minutes and with the amount of protein up to at least 1.0 mg/ml. The linearity of GSK525060 formation was also linear up to at least 150 pmol CYP3A4/ml when 10 μ M casopitant was

incubated with BactosomesTM expressing human CYP3A4 (data not shown). From these experiments the conditions which gave the best compromise between linearity of reaction and readily detectable amounts of GSK525060 were chosen; namely an incubation time of 30 minutes and an enzyme content of 0.1 mg protein/ml or 100 pmol CYP3A4/ml, for HLM and recombinant CYP3A4, respectively. Further experiments run under these conditions, with a final concentration of casopitant ranging between 0.1 to 50 μ M, indicated that casopitant metabolism followed Michaelis-Menten kinetics. The Michaelis-Menten and Linearweaver-Burk plots are reported in Figure 3 and Figure 4 for HLM and recombinant CYP3A4, respectively. In HLM the formation of GSK525060 was characterized by a K_m of 21.1 μ M and V_{max} of 65.4 pmol/pmolCYP/h. The formation of GSK525060 and of other minor metabolites of casopitant by other CYP isoforms was negligible (data not shown).

In vivo Clinical Data

Interaction of casopitant as DDI perpetrator on CYP3A4 substrates

The potential of casopitant as perpetrator of CYP3A4 interactions affecting the pharmacokinetics of co-administered drugs was investigated clinically using the two probe substrates, MID and NIF.

After repeat-dose administration of casopitant, the plasma exposure to MID increased in a dose dependent manner, an effect which may result in clinically significant pharmacologic effects, particularly with the 120 mg casopitant dose (Table 4). Thus, after repeated administration of casopitant at 30 or 120 mg/day, MID exposure as $AUC_{(0-\infty)}$

increased 2.0 and 2.7-fold after three days of casopitant administration, 1.8 and 3.5-fold with casopitant at steady-state, i.e. at 14 days of administration (Zamuner, 2010).

In the second DDI study, casopitant given at 30 and 120 mg/day significantly increased exposure of NIF by inhibiting its metabolism. The overall effect may be clinically relevant, though mild in magnitude (1.4 to 1.8-fold) (Table 4). The increases in NIF exposures appeared to be nearly comparable, regardless of the casopitant dose used and the duration of dosing.

In contrast, the pharmacokinetics of casopitant or GSK525060 were not altered by co-administration of either MID or NIF.

Interaction of CYP3A4 inhibitor or inducer with casopitant as a victim

When co-administered with the potent CYP3A4 inhibitor KET, casopitant elimination was prolonged, resulting in an increase in total exposure following a single-dose at 100 mg (Johnson, 2010). In particular, the exposure $AUC_{(0-t)}$ was increased of at least 12.1-fold and C_{max} by about 2.7-fold (Table 5). The metabolism of GSK525060 and associate PK parameters were also affected. In particular, metabolite median t_{max} was delayed from 2 to 48 hours, and its exposure as $AUC_{(0-t)}$ increased by 3.7-fold. The C_{max} of GSK525060 was approximately 45% lower (ratio = 0.55) following administration of KET than when casopitant was administered alone.

Co-administration of casopitant with the CYP3A4 inducer RIF resulted in decreased plasma concentrations of both casopitant and GSK525060. Following daily dosing with RIF, casopitant exposure (after a single dose of 150 mg) was greatly decreased with $AUC_{(0-t)}$ and C_{max} reduced by 96% (ratio = 0.039) and 89% (ratio = 0.11), respectively

(Table 6). Similarly, systemic exposure to GSK525060 as $AUC_{(0-t)}$ (after casopitant and RIF co-administration) was decreased by 94% (ratio = 0.057), whilst t_{max} of both casopitant and GSK525060 were not affected by the presence of RIF.

SimCypTM Simulations

Simulated plasma concentration-time profiles and pharmacokinetic parameters for a single oral dose of casopitant at 100 mg were consistent with the reported clinical pharmacokinetic studies (Table 7) and support the model and the parameters used for the SimCypTM simulations.

$AUC_{(0-t)}$ ratios for the simulated interaction between casopitant at 30 and 120 mg and MID or NIF are given in Table 4. The mean $AUC_{(0-t)}$ for MID was predicted to increase from 1.8 to 3.6-fold, while for NIF the predicted increase was from 1.6 to 3.5-fold throughout the casopitant regimen. Based on these simulations, there were no relevant differences between the two CYP3A4 probes. However, given the different degree of fraction metabolism (f_m) by CYP3A4 reported for MID and NIF (Ohno, 2007), we would have expected to have a different magnitude of interaction with casopitant. This discrepancy may reflect the inhibition potential of NIF on casopitant metabolism, NIF being itself a moderate CYP3A4 inhibitor (SimCypTM model includes a K_i value of 24 μ M into the NIF parameters).

Overall, with MID, the simulated mean exposure ($AUC_{(0-t)}$) increases were generally in agreement with mean clinical changes. Nevertheless, comparing simulations with clinical data obtained with casopitant at 30 mg after 3 or 14 days of administration, a slight overestimation of the casopitant inhibition potential by SimCypTM was observed. This

was likely due to the perpetrator profile introduced into SimCyp™ lacking any induction parameters for casopitant or any inhibition potential for GSK525060.

The simulated effects of co-administration of KET (400 mg) or RIF (600 mg) on casopitant C_{\max} and $AUC_{(0-t)}$ are given in Table 8. The mean C_{\max} and $AUC_{(0-t)}$ for casopitant at 100 mg was predicted to increase by a 2.8 and 9.1-fold, respectively, when co-administered with KET. Following repeat dosing of RIF, the systemic exposure to casopitant at 150 mg, as C_{\max} and $AUC_{(0-t)}$, was predicted to decrease by about 62% (ratio = 0.38) and 86% (ratio = 0.14), respectively. No simulation has been performed on the effect of KET or RIF on the systemic exposure of GSK525060.

DISCUSSION

The assessment of the potential for CYP3A4 mediated DDIs was an important part of the clinical development program for casopitant, due mainly to its *in vitro* profile. Further complexity was added by the fact that casopitant was under development for different clinical indications, several drug regimens, requiring acute or chronic dosing at different dose strengths, with different potential co-medications.

In vitro studies using HLM have demonstrated that casopitant inhibited CYP3A4 metabolism of the probe substrates MID and NIF with similar potencies. Moreover, casopitant showed metabolism-dependent inhibition of CYP3A4, consistently with the finding that its major metabolite, GSK525060, was itself a CYP3A4 inhibitor. Thus, the overall conclusion of all the *in vitro* studies was that both casopitant and its metabolite GSK525060 were direct and metabolism dependent CYP3A4 inhibitors. The metabolite GSK525060 was observed in plasma after single (Pellegatti, 2009), and repeated (Zamuner, 2010) oral administration of casopitant with an exposure of about the same order of magnitude as the parent compound. In addition casopitant showed a moderate induction of CYP3A4 in cultured human hepatocytes, with a response likely to be mediated by the nuclear Pregnane X Receptor (Luo, 2002; Lin, 2006). *In vivo* these two contrasting effects may vary in time with respect to each other, so that one or the other could prevail depending on the drug that was co-administered with casopitant and on the casopitant therapeutic regimen.

The *in vitro* results presented here provided the basis for the strategy to assess the role of casopitant as DDI perpetrator. Two clinical studies were conducted, using MID and NIF as probe substrates. A three-day dose regimen of oral casopitant increased MID exposure

as $AUC_{(0-t)}$ by about 2- to 3-fold (from 30 mg to 120 mg) in a dose-dependent manner. The increase in MID exposure was higher when MID was co-administered with casopitant under steady state plasma concentrations. This could be the clinical correlation of the time-dependent inhibition observed in vitro. Based on the clinical results obtained at 30 or 120 mg/day, casopitant could be considered as a moderate inhibitor of CYP3A4, according to FDA classification system (FDA, <http://www.fda.gov/downloads/Drugs/GuidanceComplianceRegulatoryInformation/Guidances/ucm072101.pdf>).

The increases in exposure caused by casopitant with respect to the CYP3A4 substrate NIF were slightly lower than that observed for MID, i.e. 1.8-fold after a three-day administration and 1.4-fold after 14 days of oral casopitant (120 mg/day). Moreover, casopitant at steady state increased NIF exposure less than after 3 days of casopitant administration, suggesting that, under conditions of protracted treatment, the induction potential of casopitant could play a role in the interaction between casopitant and NIF.

Despite the comparable in vitro IC_{50} values of casopitant on the CYP3A4-dependent metabolism of NIF compared to MID, the clinical results showed a clear difference in probe substrate sensitivity, and this may be explained by different factors: the existence of clearance pathways of the probe substrates not dependent on CYP3A4; the pharmacokinetic clinical variability observed mainly with NIF (Zamuner, 2010); or a different metabolism of the probe substrates mediated by intestinal CYP3A4, as reported by Foti, 2010 and Paine, 1997.

It is well known that MID and NIF are characterized by different kinetics, suggesting the existence of different preferential binding domain (i.e. hyperbolic inhibition for MID and

substrate inhibition for NIF, Galetin, 2003) and by different fraction of the total dose which is metabolized by CYP3A4 ($f_m=0.92$ for MID and $f_m=0.78$ for NIF, Ohno, 2007).

Overall, MID is considered to be more sensitive than NIF in providing the best assessment of potential clinical drug-drug interactions (Galetin, 2005) and this was also the case for the clinical study reported here with casopitant. Since it was impractical to examine all possible co-administered CYP3A4 substrates for potential interactions, the potential of DDI between casopitant and other co-administered drugs which are CYP3A4 substrates was estimated from the clinical data just discussed. The extent of interaction is likely to depend on the fractional clearance of the co-administered drugs, which can be attributed to CYP3A4. Thus MID given orally is very largely metabolized by CYP3A4 and will be subjected to a very significant interaction by co-administered casopitant (120 mg/day), with a 3.5-fold increase in MID exposure. Interactions may be of lower magnitude with intravenous casopitant and other intravenous administered agents, because their reduced liver concentration will show no impact on first-pass metabolism of a co-administered drug given orally (Galetin, 2010).

The clinical studies conducted to investigate the potential of casopitant as a victim of DDI were conducted with KET and RIF. Based on the consistency between K_m values measured in vitro in HLM and recombinant human CYP3A4, the latter must be the main enzyme involved in casopitant metabolism in man. The co-administration of casopitant together with KET, a potent CYP3A4 inhibitor, increased casopitant and GSK525060 exposure prolonging drugs' elimination and decreasing their metabolism. The increase in GSK525060 daily exposure observed after administration of KET suggests that CYP3A may be involved not only in the production of GSK525060 from casopitant but in its

further metabolism, too. These clinical results, finally, supported the in vitro data showing that CYP3A is primarily responsible for the metabolism and clearance of casopitant and the formation and clearance of its metabolites (Johnson, 2010; Pellegatti, 2009). Moreover, repeat oral dosing of RIF, a potent CYP3A4 inducer, significantly decreased systemic exposure of casopitant and its relevant metabolite by ~95% (Johnson, 2010).

A retrospective analysis of the DDI data was performed simulating the in vivo data using SimCypTM, a computer-based DDI tool for estimating the metabolic clearance of drugs and the effects of metabolic interactions in humans using in vitro metabolism and inhibition data (Howgate, 2006). Casopitant data were used to assess the potential of this software in the early clinical stages. For this reason, we have not included any data on GSK525060, since it was unavailable at this phase of drug development. The potential of casopitant as DDI perpetrator was conducted with MID and NIF as probe substrates.

SimCypTM was able to simulate the different degree of interaction between casopitant and MID observed after repeated administrations of casopitant, at doses of 30 or 120 mg/day. On the contrary, simulations with NIF were not in complete agreement with the clinical data, as clinically an interaction lower than predicted by the model was observed, especially when casopitant was given chronically. This discrepancy is likely due to the high variability observed in the clinical study and casopitant induction potential that was not considered in the model used (Zamuner, 2010). Moreover, the DDI predicted by SimCypTM appeared to be an overestimation, as the CYP3A4 inhibitor effect of nifedipine included in the model has not been observed in the clinical study.

The retrospective analysis of DDI potential for casopitant as victim was conducted with KET and RIF. The SimCyp™ analysis on KET interaction was generally in agreement with the clinically observed changes in casopitant exposure and pharmacokinetics. There was a trend of SimCyp™ to slightly underestimate by about 25% the clinical effect of KET on casopitant exposure as judged by the AUC. Considering the higher inter-individual variability of the simulated trials compared to that of clinical study design this difference may be considered not relevant. The simulation performed with RIF underestimated the magnitude of the interaction by about 3.5-fold. However, under steady state conditions, once the maximum extent of interaction had been reached, the simulated effect of RIF on casopitant became close to the clinical one.

Overall, the clinical data confirmed the ability of casopitant to act as a substrate, inhibitor and possibly as inducer of CYP3A4. The clinical studies conducted to investigate the potential of casopitant as DDI perpetrator confirmed that this drug was a moderate inhibitor of CYP3A4 according to the FDA classification system (FDA, <http://www.fda.gov/downloads/Drugs/GuidanceComplianceRegulatoryInformation/Guidances/ucm072101.pdf>).

The clinical studies conducted to investigate the potential of casopitant as DDI victim, suggested that co-administration of casopitant with potent inducers of CYP3A4 was likely to result in decreased efficacy and was not to be recommended. Moreover, co-administration of casopitant with strong inhibitors of CYP3A4 should be used with caution as this was likely to result in increased casopitant exposure, overcoming the toxicological cover.

In conclusion, the in vitro data were accurate and robust enough to build reliable SimCypTM models to estimate the potential DDI of casopitant and to minimize the clinical studies recommended. The approach based on the prediction of clinical data from in vitro results would eliminate the need of numerous unnecessary clinical DDI studies, especially the need to test different doses, and would eventually accelerate the availability of therapy to patients.

ACKNOWLEDGEMENTS

We thank Roberto Tolando for the co-ordination of in vitro activities and helpful discussion, Roberta Mastropasqua and Daniela Reami for HPLC/MS-MS quantification assays, and the entire casopitant Clinical Pharmacology team for the design, conduct, and analysis of the clinical studies, and in particular Brendan Johnson for scientific support. We also appreciate Professor Francesco De Matteis for the useful discussion on this topic.

AUTHORSHIP CONTRIBUTIONS

Participated in research design: Motta, Pons, Pagliarusco, and Bonomo.

Conducted experiments: Pons.

Performed data analysis: Pons, and Bonomo.

Wrote or contributed to the writing of the manuscript: Motta, Pons, Pagliarusco, Pellegatti, and Bonomo.

REFERENCES

Bibi Z (2008) Role of cytochrome P450 in drug interactions. *Nutrition & Metabolism* **5**:27-36.

Ekins S, Stresser DM, and Andrew Williams J (2003) In vitro and pharmacophore insights into CYP3A4 enzymes. *Trends Pharmacol Sci* **24**:161-166.

Fahmi OA, Boldt S, Kish M, Obach RS, and Tremaine LM (2008) Prediction of Drug-Drug Interactions from In vitro Induction data. *Drug Metab Dispos* **36**:1971-1974.

Fahmi OA, Hurst S, Plowchalk D, Cook J, Guo F, Youdim K, Dickins M, Phipps A, Darekar A, Hyland R, and Obach RS (2009) Comparison of Different Algorithms for Predicting Clinical Drug-Drug Interactions, Based on the Use of CYP3A4 In Vitro Data: Predictions of Compounds as Precipitants of Interaction. *Drug Metab Dispos* **37**:1658-1666.

Foti RS, Rock DA, Wienkers LC, and Wahlstrom JL (2010) Selection of Alternative CYP3A4 Probe Substrates for Clinical Drug Interaction Studies Using In Vitro Data and In Vivo Simulation. *Drug Metab Dispos* **38**:981-987.

Galetin A, Clarke SE, and Houston JB (2003) Multisite Kinetic Analysis of Interactions between Prototypical CYP3A4 Subgroup Substrates: Midazolam, Testosterone, and Nifedipine. *Drug Metab Dispos* **31**:1108-1116.

Galetin A, Ito K, Hallifax D, and Houston JB (2005) CYP3A4 Substrate Selection and Substitution in the Prediction of Potential Drug-Drug Interactions. *J Pharmacol Exp Ther* **314**:180-190.

Galetin A, Gertz M, and Houston JB (2010) Contribution of Intestinal Cytochrome P450-Mediated Metabolism to Drug-Drug Inhibition and Induction Interactions. *Drug Metab Pharmacokinet* **25**:28-47.

Herrstedt J, Apornwirat W, Shaharyar A, Aziz Z, Roila F, Van Belle S, Russo MW, Levin J, Ranganathan S, Guckert M, and Grunberg SM (2009) Phase III trial of casopitant, a novel neurokinin-1 receptor antagonist, for the prevention of nausea and vomiting in patients receiving moderately emetogenic chemotherapy. *J Clin Oncol* **27**:5363-5369.

Hewitt NJ, Lecluyse EL, and Ferguson SS (2007) Induction of hepatic cytochrome P450 enzymes: methods, mechanisms, recommendations, and in vitro in vivo correlations. *Xenobiotica* **37**:1196-1224.

Howgate EM, Rowland Yeo K, Proctor NJ, Tucker GT, and Rostami-Hodjegan A (2006) Prediction of in vivo drug clearance from in vitro data. Impact of inter-individual variability. *Xenobiotica* **36**:473-497.

Johnson BM, Adams LM, Zhang K, Gainer SD, Kirby LC, Blum RA, Apseloff G, Morrison RA, Shutz RA, and Lebowitz PF (2010) Ketokonazole and Rifampin Significantly Affect the Pharmacokinetics, But Not the Safety or QTc Interval, of Casopitant, a Neurokinin-1 Receptor Antagonist. *J Clin Pharmacol* **50**:951-959.

LeCluyse EL (2001) Human hepatocyte culture systems for the in vitro evaluation of cytochrome P450 expression and regulation. *Eur J Pharm Sci* **13**:343-368.

Lin JH (2006) CYP induction-mediated drug interactions: in vitro assessment and clinical implications. *Pharm Res* **23**:1089-1115.

Luo G, Cunningham M, Kim S, Burn T, Lin J, Sinz M, Hamilton G, Rizzo C, Jolley S, Gilbert D, Downey A, Mudra D, Graham R, Carroll K, Xie J, Madan A, Parkinson A, Christ D, Selling B, Lecluyse E, and Gan LS (2002) CYP3A4 induction by drugs: correlation between a Pregnane x Receptor reporter gene assay and CYP3A4 expression in human hepatocytes. *Drug Metab Dispos* **30**:795-804.

Madan A, Usuki E, Burton L, Ogilvie B, Parkinson A (2002) *In Vitro* Approaches for Studying the Inhibition of Drug-Metabolizing Enzymes and Identifying the Drug-Metabolizing Enzymes Responsible for the Metabolism of Drugs, in *Drug-Drug Interactions* (Rodriguez A ed.), pp 217-294, Marcel Dekker, Inc., New York.

Madan A, Graham RA, Carroll KM, Mudra DR, Burton A, Krueger LA, Downey AD, Czerwinski M, Forster J, Ribadeneira MD, Gan LS, LeCluyse E, Zech K, Robertson P, Koch P, Antonian L, Wagner G, Yu L, and Parkinson A (2003). Effect of prototypical microsomal enzyme inducers on cytochromes P450 expression in cultured human hepatocytes. *Drug Metab Dispos* **31**:421-431.

Maurel P (1996) The use of adult human hepatocytes in primary culture and other in vitro systems to investigate drug metabolism in man. *Adv Drug Del Rev* **22**:105-132.

Minthorn E, Mencken T, King AG, Shu A, Rominger D, Gontarek RR, Han C, Bambal R, and Davis CB (2008) Pharmacokinetics and Brain Penetration of Casopitant, a Potent and Selective Neurokinin-1 Receptor Antagonist, in the Ferret. *Drug Metab Dispos* **36**:1846-1852.

Ohno Y (2007) General Framework for the Quantitative Prediction of CYP3A4-Mediated Oral Drug Interactions Based on the AUC Increase Coadministration of Standard Drugs. *Clin Pharmacokinet* **46**:681-696.

Paine MF, Khalighi M, Fisher JM, Shen DD, Kunze KL, Marsh CL, Perkins JD, and Thummel KE (1997) Characterization of Interintestinal and Intraintestinal Variations in Human CYP3A-Dependent Metabolism. *J Pharmacol Exp Ther* **283**:1552-1562.

Pellegatti M, Bordini E, Fizzotti P, Roberts A, and Johnson BM (2009) Disposition and Metabolism of Radiolabeled Casopitant in Humans. *Drug Metab Dispos* **37**:1635-1645.

Polasek TM, and Miners JO (2007) In vitro approaches to investigate mechanism-based inactivation of CYP enzymes. *Exp Opin Drug Metab Toxicol* **3**:321-329.

Sinz M, Wallace G, and Sahi J (2008) Current industrial practises in assessing CYP450 enzyme induction: preclinical and clinical. *AAPS J* **10**:391-400

Wienkers LC, and Heath TG (2005) Predicting in vivo drug interactions from in vitro drug discovery data. *Nat Rev Drug Discov* **4**:825:833.

Xu L, Chen Y, Pan Y, Skiles GL and Shou M (2009) Prediction of human drug-drug interactions for time-dependent inactivation of CYP3A4 in primary hepatocytes using a population-based simulator. *Drug Metab Dispos* **37**:2330-2339.

Yang J, Jamei M, Yeo KR, Tucker GT, and Rostami-Hodjegan A (2005) Kinetic values for mechanism-based enzyme inhibition: Assessing the bias introduced by the conventional experimental protocol. *Eur J of Pharm Sci* **26**:334-340.

Zamuner S, Johnson BM, Pagliarusco S, Fina O, Peroni M, Fiore M, Adams LM, and Fernandes AS (2010) Effect of Single and Repeat Doses of Casopitant on the

DMD # 35071

Pharmacokinetics of CYP450 3A4 Substrates Midazolam and Nifedipine. *Br J Clin Pharmacol* **70**:537-546.

LEGENDS FOR FIGURES

Figure 1 Chemical structure of GW679769 and its metabolite GSK525060.

Figure 2 Determination of K_I and k_{inact} for the metabolism-dependent inhibition of CYP3A4 by casopitant in HLM. Upper panel shows the time- and concentration-dependent inactivation of CYP3A4 by casopitant expressed as the percentage of control enzyme activity versus time; lower panel represents the plot of the observed inactivation rate constants (k_{obs}) versus casopitant concentration. Each concentration of casopitant was tested in duplicate and kinetic constants (K_I and k_{inact}) were determined by non-linear regression: $K_I = 3.1 \pm 1.6 \mu\text{M}$ (\pm standard error) and $k_{\text{inact}} = 0.0199 \pm 0.0024 \text{ min}^{-1}$ (\pm standard error).

Figure 3 Michaelis-Menten and Linearweaver-Burk (insert) plots for the conversion of casopitant to GSK525060 by human liver microsomes. Each concentration of casopitant was tested in triplicate and kinetic parameters were determined: $K_m = 21.1 \pm 2.2 \mu\text{M}$ (\pm standard error) and $V_{\text{max}} = 65.4 \pm 3.0 \text{ pmol/pmolCYP/h}$ (\pm standard error).

Figure 4 Michaelis-Menten and Linearweaver-Burk (insert) plots for the conversion of casopitant to GSK525060 by recombinant human CYP3A4. Each concentration of casopitant was tested in triplicate and kinetic parameters were determined: $K_m = 10.1 \pm 2.5 \mu\text{M}$ (\pm standard error) and $V_{\text{max}} = 81.9 \pm 7.4 \text{ pmol/pmolCYP/h}$ (\pm standard error).

TABLES**Table 1** Physicochemical and pharmacokinetic input parameters used in SimCyp™ simulation for casopitant.

Parameters	Values	Parameters	Values
Molecular weight	616.6	F _{u, gut}	1
LogP	5.6	F _{u, mic}	0.05
pK _a	6.3	V _{ss} (l kg ⁻¹)	2.58
Blood/plasma ratio (B/P)	0.61	Cl _{int} HLM (μL/min/mg protein)	25
F _{u, p} (plasma)	0.005	K _i (μM)	4.93
F _a	~ 0.93	CYP3A4 k _{inact} (min ⁻¹)	0.0199
K _a (h ⁻¹)	4.1	CYP3A4 K _I (μM)	3.1
Q _{gut} (l h ⁻¹)	~ 1	f _m CYP3A4	~ 1

F_{u, mic} fraction unbound in microsomes (predicted by SimCyp™ at 1 mg/ml protein); f_{u, p} unbound fraction of drug in plasma; B:P blood: plasma concentration ratio (in-house data); F_a fraction of drug absorbed (calculated from clinical radiolabel study as reported by Pellegatti, 2009); K_a scaled from in vivo clearance of clinical intravenous study, in-house data; Q_{gut} intestinal blood flow predicted by SimCyp™; V_{ss} assuming a 75 kg volunteer (calculated from clinical radiolabel study as reported by Pellegatti, 2009); Cl_{int} HLM calculated as K_m/V_{max}; K_i value estimated as IC₅₀ calculated value on MID/2; f_m CYP3A4, fraction of drug metabolized by CYP3A4 ; k_{deg} provided by SimCyp™ was 0.000128 min⁻¹; unless indicated otherwise, other inputs are in-house calculated values.

Table 2 Effect of Casopitant and Prototypical CYP Inducers on CYP3A4 activity (Testosterone 6 β -hydroxylase) Following Incubation in Cultured Human Hepatocytes for 3 Days.

Treatment	Mean activity ^a (nmol/min/mg)	Inductive Response as Fold Change (and % positive control)	Mean activity ^a (nmol/min/mg)	Inductive Response as Fold Change (and % positive control)	Mean activity ^a (nmol/min/mg)	Inductive Response as Fold Change (and % positive control)
	Donor 1		Donor 2		Donor 3	
Control ^b	4.5	1.0	1.7	1.0	7.2	1.0
Rifampin ^c	9.7	2.1 (100)	22	13 (100)	43	6.0 (100)
Phenobarbital ^c	12	2.7 (150)	16	9.4 (70)	44	6.1 (101)
Omeprazole ^c	4.9	1.1 (6.8)	6.4	3.8 (24)	17	2.3 (27)
1 μ M casopitant	4.7	1.0 (4.1)	4.7	2.8 (15)	14	2.0 (19)
5 μ M casopitant	5.2	1.1 (13)	12	7.2 (52)	20	2.7 (34)
20 μ M casopitant	3.1	0.70 (NA)	9.6	5.7 (40)	14	1.9 (18)

a. Values are expressed as a mean of 2 replicates.

b. Controls received 0.1% (v/v) DMSO only.

c. Prototypical CYP Inducers are: 10 μ M Rifampin, 500 μ M Phenobarbital and 25 μ M Omeprazole.

NA Not applicable since the basal activity is greater than that with casopitant 20 μ M and the % positive control becomes a negative value.

Table 3 CYP3A4 inhibition in human liver microsomes by casopitant and GSK525060.

	Probe substrate	Direct Inhibition IC₅₀ (μM) ± SE	Metabolism dependent inhibition IC₅₀ fold change
Casopitant	Midazolam	9.86 ± 1.78	4.27
	Nifedipine	9.72 ± 1.18	3.37
GSK525060	Midazolam	8.22 ± 2.76	2.96
	Nifedipine	5.60 ± 0.45	13.7

SE: Standard Error provided by Grafit.

Table 4 Effects of co-administration of casopitant on AUC of CYP3A4 substrates, midazolam (oral dosed at 5 mg) and nifedipine (oral dosed at 10 mg): comparison of clinical results and SimCypTM simulations.

Substrate	Casopitant dose and regimen	Substrate AUC _(0-∞) fold change ^a	
		Clinical ratio ^{b, c}	Predicted ratio ^d
Midazolam	30 mg (once daily x 3)	2.02 (1.75-2.32)	1.77 (1.29-2.53)
Midazolam	30 mg (once daily x 14)	1.76 (1.53-2.03)	2.12 (1.34-3.36)
Midazolam	120 mg (once daily x 3)	2.67 (2.18-3.27)	2.46 (1.49-3.96)
Midazolam	120 mg (once daily x 14)	3.49 (2.98-4.08)	3.57 (1.65-7.75)
Nifedipine	30 mg (once daily x 3)	1.56 (1.37-1.78)	1.61 (1.24-2.12)
Nifedipine	30 mg (once daily x 14)	1.61 (1.39-1.87)	1.94 (1.32-2.77)
Nifedipine	120 mg (once daily x 3)	1.77 (1.54-2.04)	2.35 (1.53-3.40)
Nifedipine	120 mg (once daily x 14)	1.42 (1.23-1.65)	3.45 (1.68-6.55)

- a Exposure ratios are given with two decimal places in tables, and with at least one decimal place in the text.
b Ratios from clinical data are expressed as geometric mean ratio with 90% CI given in parentheses.
c Reference: Zamuner, 2010.
d Ratios from simulations are expressed as geometric mean ratio with the 90% CI given in parentheses.

Table 5 Summary Statistics of casopitant and GSK525060 PK Parameters when casopitant was co-administered with ketoconazole: Mean \pm Standard Deviation – median and range for t_{\max} .

Analyte	Treatment ^{c, d}	AUC _(0-t) (ng.h/ml)	C _{max} (ng/ml)	t _{max} (h)
Casopitant	A	2590 \pm 572	457 \pm 68	1.00 (0.50-2.50)
	B	31200 \pm 7570	1250 \pm 254	2.00 (1.00-2.53)
	Ratio treatment B vs. A ^{a, b}	12.10 ^f	2.71	
GSK525060	A	2470 \pm 451	245 \pm 40	2.00 (1.00-2.50)
	B	9150 \pm 2250	135 \pm 30	47.92 (23.92-96.00)
	Ratio treatment B vs. A ^{a, b}	3.66 ^e	0.55	

- a. Exposure ratios are given with two decimal places in tables, and with at least one decimal place in the text.
b. Reference: Johnson, 2010.
c. Treatment A = 100 mg oral casopitant (n = 13).
d. Treatment B = 100 mg oral casopitant (Day 4) + 400 mg ketoconazole (QD, Day 1 to Day 7) (n = 13).
e. Comparison based on geometric mean of AUC_(0-t).

Table 6 Casopitant and GSK525060 PK Parameters observed when casopitant is either administered on its own or together with rifampin: Mean \pm Standard Deviation – median and range for t_{\max} .

Analyte	Treatment ^{c,d}	AUC _(0-t) (ng.h/ml)	C _{max} (ng/ml)	t _{max} (h)	t _{1/2} (h)
Casopitant	A	6570 \pm 2180	847 \pm 279	1.25 (0.53-6.00)	19.2 \pm 7.1
	B	273 \pm 127	93.2 \pm 39.8	1.00 (0.50-2.05)	6.45 \pm 2.95
	Ratio treatment B vs. A ^{a,b}	0.04 ^e	0.11		
GSK525060	A	5260 \pm 1380	350 \pm 110	2.00 (1.00-8.00)	17.6 \pm 7.0
	B	311 \pm 114	93.0 \pm 32.2	1.26 (0.50-2.05)	3.36 \pm 1.12
	Ratio treatment B vs. A ^{a,b}	0.06 ^e	0.26		

- a. Exposure ratios are given with two decimal places in tables, and with at least one decimal place in the text.
b. Reference: Johnson, 2010.
c. Treatment A = 150 mg oral casopitant (N = 18).
d. Treatment B = 150 mg oral casopitant (Day 8) + 600 mg rifampin (QD, Day 1 to Day 9) (N = 16).
e. Comparison based on geometric mean of AUC_(0-t).

Table 7 Casopitant pharmacokinetics after a single oral dose at 100 mg: comparison of clinical results and SimCyp™ simulations.

Casopitant (mg)	Casopitant C _{max} (ng/ml)		Casopitant AUC (ng.h/ml)	
	Clinical mean ^a	Predicted mean ^b	Clinical mean ^a	Predicted mean ^b
100	457 (415-498)	340 (140-650)	2590 (2240-2930)	4760 (2350-8610)

a. Exposure clinical data are given with the 90% CI given in parentheses.

b. Predicted data are data generated by SimCyp™, with the 90% CI given in parentheses.

Table 8 Effects of co-administration of CYP3A4 inhibitor (ketoconazole oral dosed at 400 mg) or CYP3A4 inducer (rifampin oral dosed at 600 mg/day) on casopitant pharmacokinetics: comparison of clinical results and SimCyp™ simulations.

Casopitant (mg)	Perpetrator	Casopitant C _{max} fold change ^a		Casopitant AUC fold change ^a	
		Clinical mean ^{c,d}	Predicted mean ^b	Clinical mean ^{c,d}	Predicted mean ^b
100	Ketoconazole	2.71 (2.39-3.06)	2.82 (2.73-3.00)	12.1 (11.00-13.20)	9.14 (2.74-24.30)
					33.30 (13.20-86.60) SS
150	Rifampin	0.11 (0.08-0.14)	0.38 (0.03-0.47)	0.040 (0.03-0.05)	0.14 (0.04-0.31)
					0.05 (0.01-0.09) SS

a. Exposure ratios are given with two decimal places in tables, and with at least one decimal place in the text.

b. Predicted comparisons are data generated by SimCyp™, based on geometric mean of AUC_(0-t), with the 90% CI given in parentheses; SS steady state conditions.

c. Clinical comparisons are data based on geometric mean of AUC_(0-t), with the 90% CI given in parentheses.

d. Reference: Johnson, 2010.

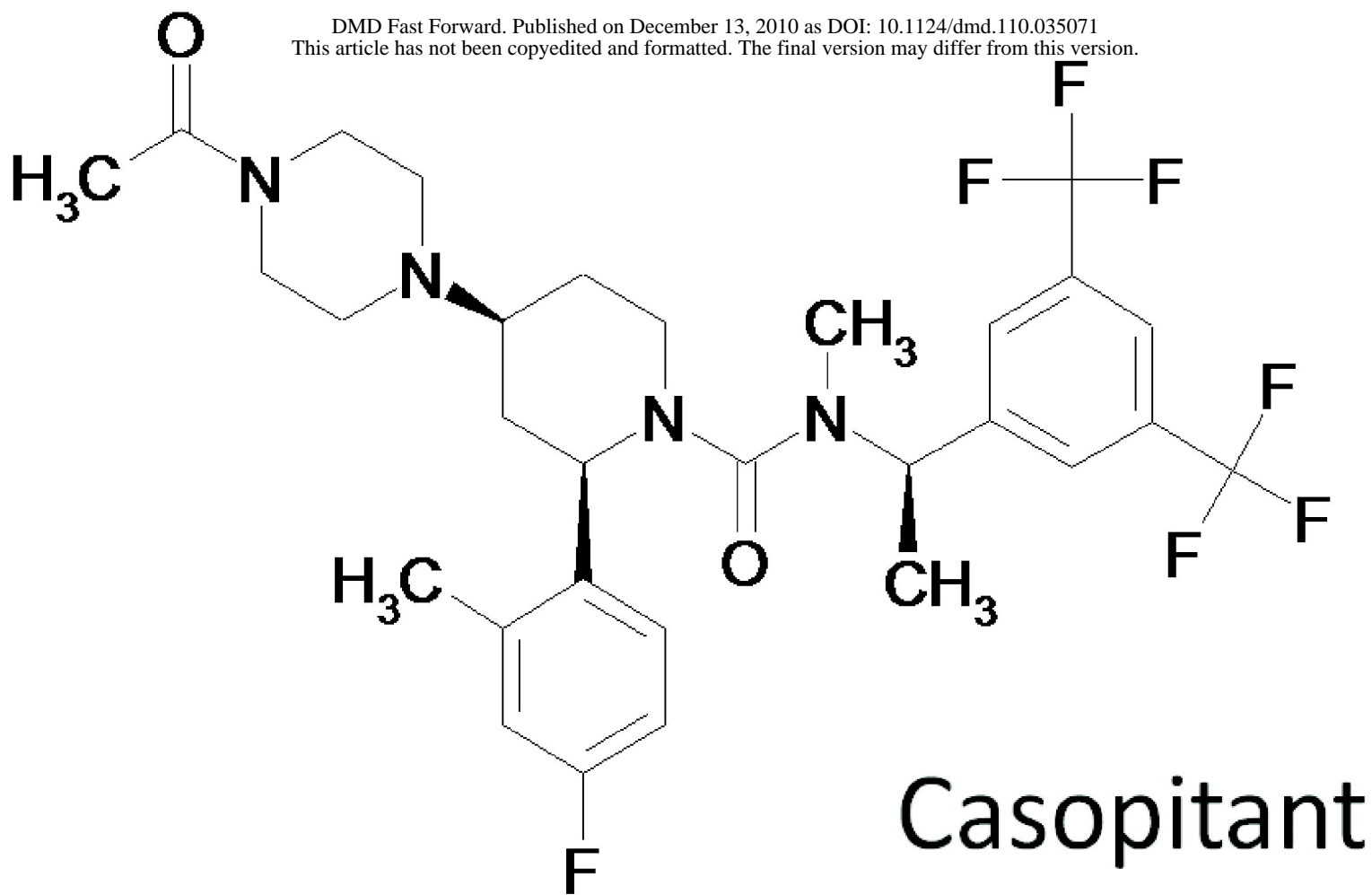
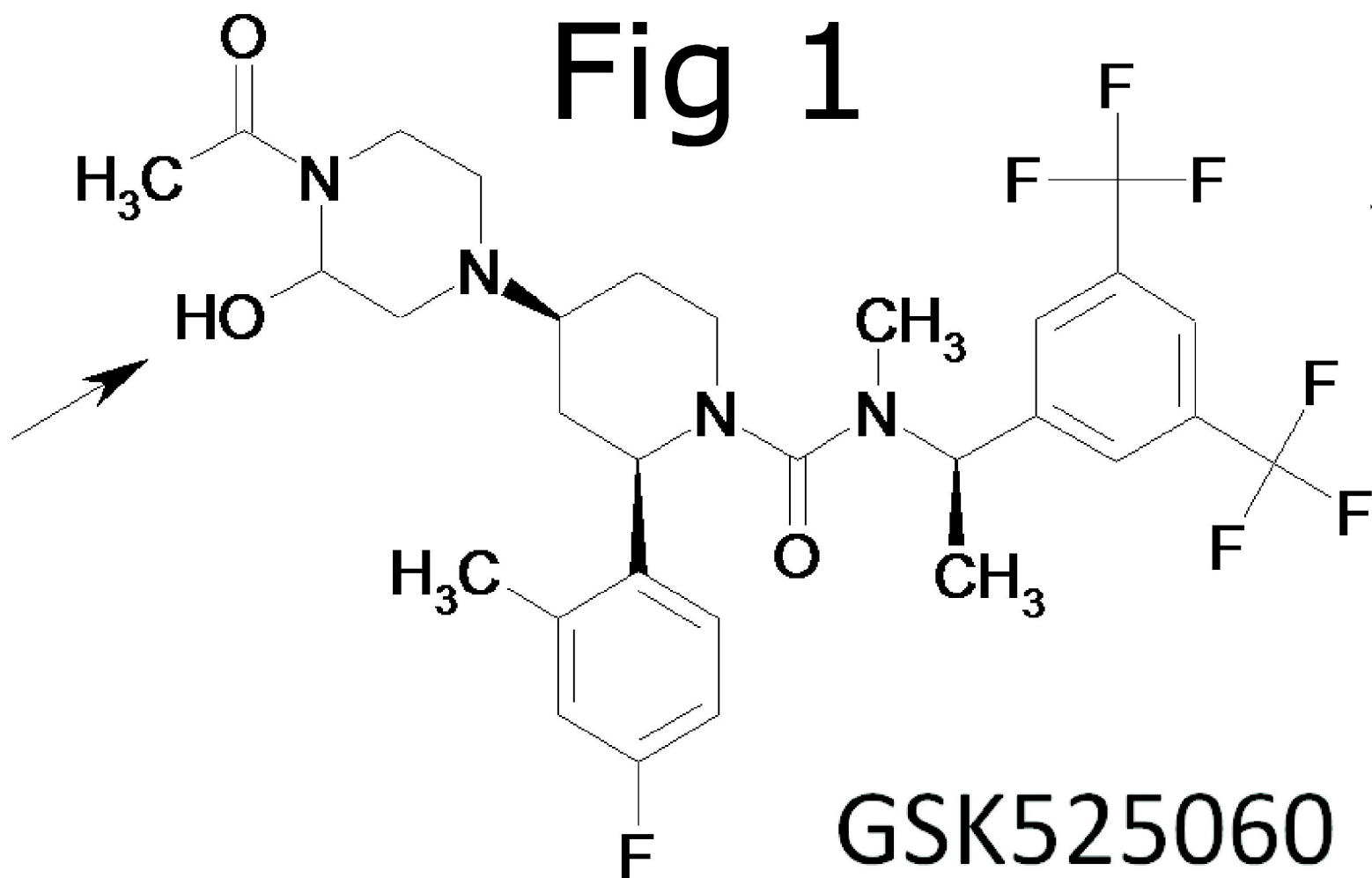


Fig 1



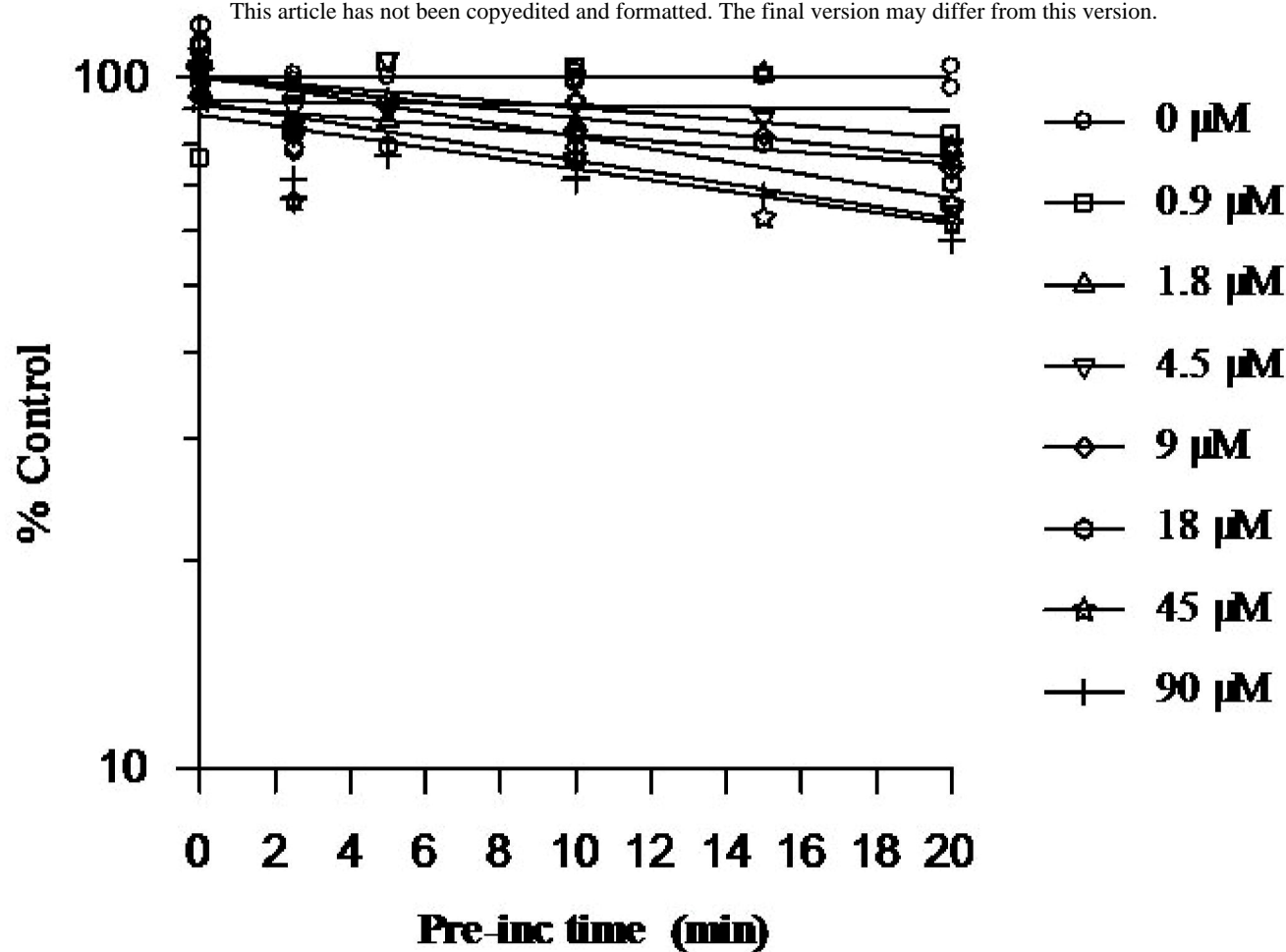
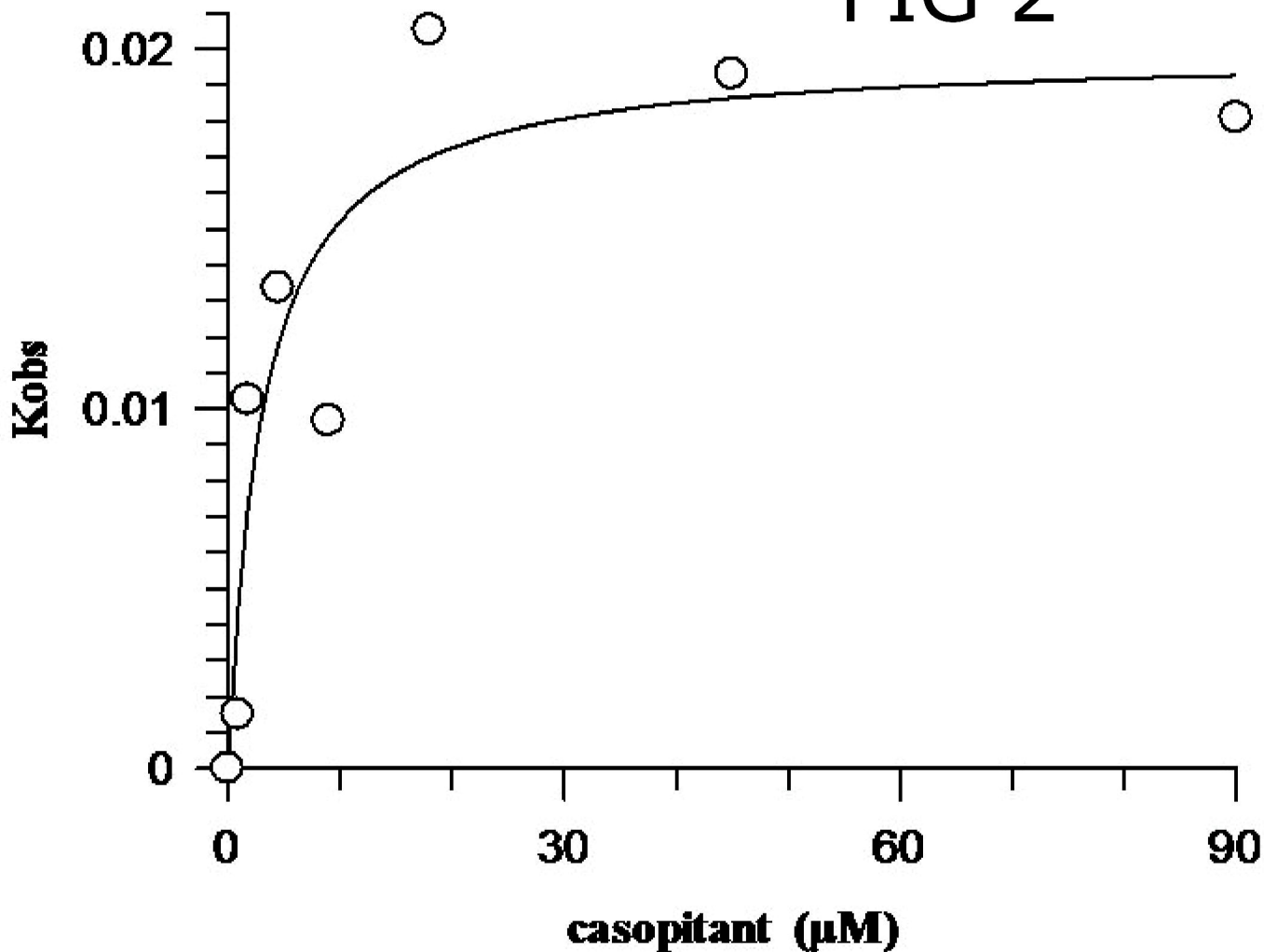
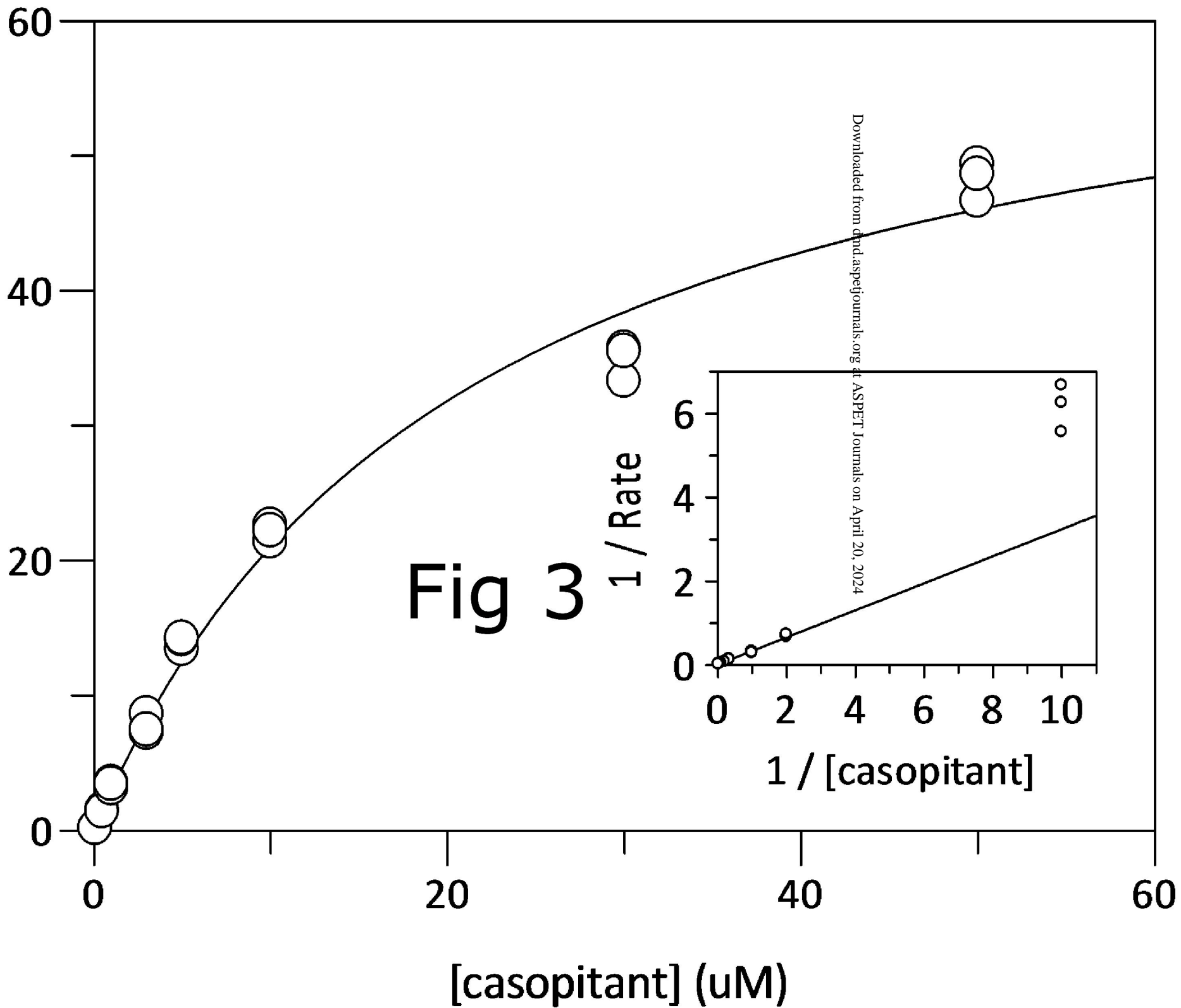


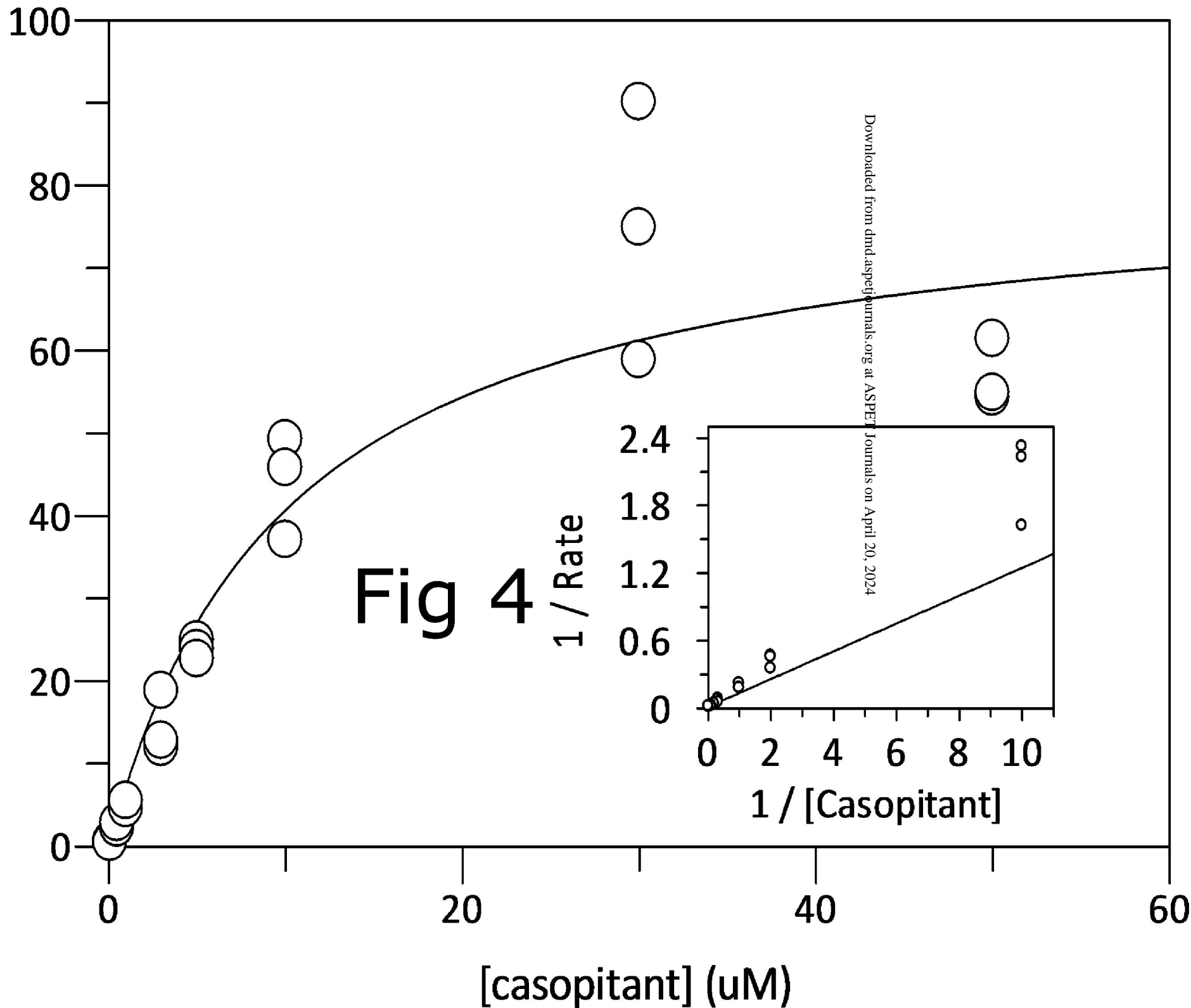
FIG 2



GSK525060 formation
(pmol/pmolCYP/h)



GSK525060 formation
(pmol/pmolCYP/h)



Downloaded from dmnd.aspetjournals.org at ASPET Journals on April 20, 2024